I. Troch, F. Breitenecker, eds. ISBN 978-3-901608-35-3

NONLINEAR MODELING AND ANALYSIS OF AIRCRAFT GROUND DYNAMICS

J. Rankin[1], B. Krauskopf[1], M. Lowenberg[1] and E. Coetzee[2]
[1]University of Bristol, UK [2]Landing Gear Systems, Airbus, UK

Corresponding author: James Rankin, Department of Engineering Mathematics,
Faculty of Engineering, University of Bristol, Bristol, UK, BS8 1TR
Email: j.rankin@bris.ac.uk

Abstract. The ground dynamics of passenger aircraft are influenced by nonlinear characteristics of components, especially aerodynamic surfaces and tyre properties. We present a mathematical model of a mid-sized passenger aircraft that captures these effects and apply dynamical systems tools to its study. Specifically, we present a two-parameter bifurcation analysis where we vary the steering angle and taxiway friction coefficient as parameters. Solutions are represented as surfaces that allow us to draw conclusions on the robustness of ground operations under varying operating conditions.

1 Introduction

The primary goal for commercial aircraft taxiing between terminal and runway is to do so quickly and safely. The desire to understand how this can be achieved reliably motivates the study of aircraft ground dynamics. Computer modeling can be used to gain useful insights into operational procedure of existing aircraft and help with the design of future aircraft at relatively low cost. Indeed, computer simulation has previously been used to study the dynamics of aircraft on the ground; examples are, a study of a linearised bicycle model [1] and a study of a model implemented in the multibody systems package SIMPACK that includes nonlinear effects [2]. Nonlinearities play a significant role in the dynamics of aircraft, specifically in components such as the tyres and aerodynamics. Therefore, in the development of a computer model, it is important to incorporate and evaluate nonlinearities inherent in the various components. A previous study by the authors [3] used a nonlinear model implemented in the multibody systems package SimMechanics. In contrast to previous work, the system was analysed with tools from nonlinear dynamics, specifically, a bifurcation analysis was performed.

In order to improve computational efficiency and functionality with tools used for bifurcation analysis we present here a fully mathematical description in the form of a tricycle model of a typical medium sized single aisle aircraft in which the nose wheel is used for steering. The equations of motion are given in terms of a set of ordinary differential equations, where the aircraft is modeled as a rigid body with six degrees of freedom. The forces applied to the body by components such as the tyres and aerodynamics are modeled from real test data. The model has been fully validated against the well established industry tested model used in our previous study [3].

To illustrate the use of nonlinear modeling and dynamical systems tools in the study of aircraft ground dynamics we present a bifurcation analysis with the continuation package AUTO [4]. Specifically, we investigate the effect that differences in taxiway surface condition have on the lateral stability of turning. The results are presented in terms of two-parameter bifurcation diagrams in which the solutions are represented as surfaces. The results confirm that turns made in low friction (wet) conditions can result in a loss of lateral stability at lower velocities. However, at high velocities where aerodynamic effects play a more significant role, we find that, counter intuitively, regions of stability may be extended in low friction conditions.

2 The Model

The model presented and studied here was developed from an industry-tested SimMechanics model of a typical medium sized single-aisle passenger aircraft used in a previous study [3]. The main difference between the two models is that here we do not include the effects of the aircraft's oleos (shock absorbers). We now give the equations of motion for the newly developed mathematical model and a brief overview of the modeling of individual components. The new model has been fully validated against the existing SimMechanics model.

The aircraft modeled has a tricycle configuration in which the nose gear is used for steering. We

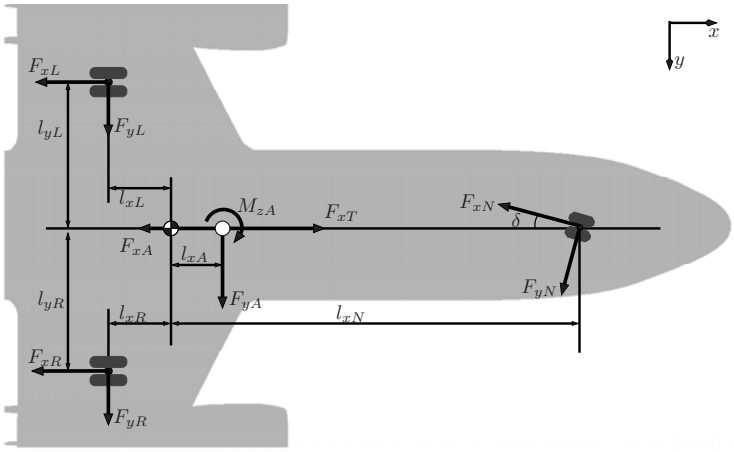

Figure 1: Schematic diagram showing relative positions of force elements F_* acting on the airframe at relative distances l_* from the CG-position (checkered circle); shown is the projection in the (x,z)-plane.

model the aircraft as a single rigid body with six degrees of freedom (DOF); three translational DOF and three rotational DOF. Throughout this study we use one of the conventionally accepted coordinate systems for aircraft. Specifically, the positive x-axis points towards the nose of the aircraft, the z-axis is the downward normal to the (flat) ground and the y-axis completes the right-handed coordinate system. This body coordinate system is assumed to coincide with the aircraft's principal axes of inertia. The equations of motion were derived from Newton's Second Law by balancing either the forces or moments in each DOF [5].

In Figure 1 the relative positions and directions of the force elements that act on the aircraft are shown in a top-down view, the (x,z)-plane in the body coordinate system. This diagram illustrates how the equations of motion are derived by balancing force elements along the x-axis and y-axis of the aircraft, and moment elements about the z-axis of the aircraft. The remaining equations are obtained by the same method but using different projections. The equations of motion for the velocities in the body-axis of the aircraft are given as six ordinary differential equations:

$$m(\dot{V}_x + V_z W_y - V_y W_z) = F_{xT} - F_{xR} - F_{xL} - F_{xN}\cos(\delta) - F_{yN}\sin(\delta) - F_{xA}, \quad (1)$$

$$m(\dot{V}_y + V_x W_z - V_z W_x) = F_{yR} + F_{yL} + F_{yN}\cos(\delta) - F_{xN}\sin(\delta) + F_{yA}, \quad (2)$$

$$m(\dot{V}_z + V_y W_x - V_x W_y) = F_{zW} - F_{zR} - F_{zL} - F_{zN} - F_{zA}, \quad (3)$$

$$\begin{aligned} I_{xx}\dot{W}_x - (I_{yy} - I_{zz})W_y W_z = {} & l_{yL}F_{zL} - l_{yR}F_{zR} - l_{zL}F_{yL} - l_{zR}F_{yR} - \\ & l_{zN}F_{yN}\cos(\delta) + l_{zN}F_{xN}\sin(\delta) + l_{zA}F_{yA} + M_{xA}, \end{aligned} \quad (4)$$

$$\begin{aligned} I_{yy}\dot{W}_y - (I_{zz} - I_{xx})W_x W_z = {} & l_{xN}F_{zN} - l_{zN}F_{xN}\cos(\delta) - l_{zN}F_{yN}\sin(\delta) - \\ & l_{xR}F_{zR} - l_{zR}F_{xR} - l_{xL}F_{zL} - l_{zL}F_{xL} + \\ & l_{zT}F_{xT} + l_{zA}F_{xA} + l_{xA}F_{zA} + M_{yA}, \end{aligned} \quad (5)$$

$$\begin{aligned} I_{zz}\dot{W}_z - (I_{xx} - I_{yy})W_x W_y = {} & l_{yR}F_{xR} - l_{yL}F_{xL} - l_{xR}F_{yR} - l_{xL}F_{yL} + \\ & l_{xN}F_{yN}\cos(\delta) - l_{xN}F_{xN}\sin(\delta) + l_{xA}F_{yA} + M_{zA}. \end{aligned} \quad (6)$$

The mass of the aircraft is set to $m = 45420$kg, a light operating case, and we use principal moments of inertia I_{xx}, I_{yy} and I_{zz} that correspond to this mass. The steering angle is applied to the nose gear and denoted δ. The velocities along each of the aircraft's axes are given by V_* and the rotational velocities about the axes by W_*. A dot notation is used to show the first derivative with respect to time of these states. The weight of the aircraft acting at the centre of gravity (CG) position is denoted $F_{zW} = mg$ and is assumed to act along the z-axis in the aircraft body coordinate system because the pitch and roll angles remain relatively small in this analysis. The thrust value used here is $F_{xT} = 28913$N which represents 13% of the maximum available thrust. The orthogonal force elements on each of the nose, main right and main left tyres are denoted F_{*N}, F_{*R} and F_{*L}, respectively. The individual aerodynamic force and moment elements act at the aerodynamic centre of the aircraft and are denoted F_{*A} and M_{*A}, respectively. The thrust force is assumed to act parallel the x-axis of the aircraft and it is denoted F_{xT}. The dimensions l_* are shown to scale in Figure 1 to give an idea of the relative lengths between

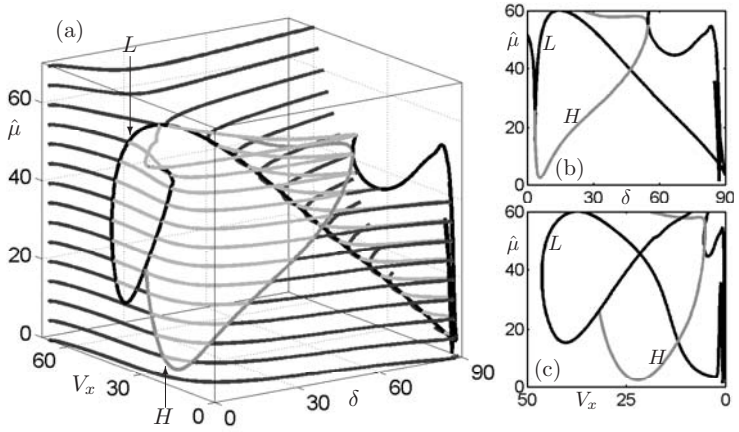

Figure 2: Panel (a) shows a surface plot of solutions in $(\delta, V_x, \hat{\mu})$-space; stable solutions are black and unstable solutions are grey. The curve of limit point bifurcations L is the thick black curve and the curve of Hopf bifurcations H is the thick grey curve. Panels (b) and (c) show two-dimensional projections of the bifurcation curves onto the $(\delta, \hat{\mu})$-plane and $(V_x, \hat{\mu})$-plane, respectively.

components.

The tyre and aerodynamic models as used here have also been used in a previous study[3] and were developed by a GARTEUR action group investigating ground dynamics [6]. Specifically, the lateral forces on the tyres depend nonlinearly on the load on the tyre and its slip angle. The aerodynamic forces depend nonlinearly on the aircraft sideslip angle, angle of attack and forward velocity; the model is based on wind-tunnel data and results from computational fluid dynamics.

3 Bifurcation Analysis of Turning Solutions

In our model fixed-radius turning circles correspond to steady-states of the system. The analysis focuses on how (steady-state) turning circle solutions change under variation of parameters. The steering angle δ and the percentage reduction in friction at the tyre-ground interface $\hat{\mu}$ are varied as parameters. At $\hat{\mu} = 0\%$ the taxiway surface conditions are considered to be normal/dry and when $\hat{\mu}$ is increased the lateral force that can be generated by the tyres reduces. A value of $\hat{\mu} = 50\%$ is considered to represent a wet taxiway and the force that the tyres can generate reduces to 0 at $\hat{\mu} = 100\%$. The results are represented as a surface of solutions that describes the dynamics over the entire range of δ and $\hat{\mu}$ as represented by a state variable, the longitudinal velocity of the aircraft V_x.

One-parameter continuation runs in δ were computed for discrete values of $\hat{\mu}$. When plotted together in $(\delta, V_x, \hat{\mu})$-space the individual bifurcation curves form a surface of solutions. Two-parameter continuation was used to compute the loci of bifurcations continuously under the variation of both δ and $\hat{\mu}$. Combining the results from these two computations into a single plot is an effective way of representing the behaviour over the complete range of δ and $\hat{\mu}$ in a single figure. Two-dimensional projections of bifurcation curves show certain features more clearly.

Figure 2(a) shows the resulting surface plot of solutions in $(\delta, V_x, \hat{\mu})$-space. Changes in stability occur at bifurcation curves on the surface, namely along the curve L of limit point bifurcations and the curve H of Hopf bifurcations. Hopf bifurcations are typically associated with the onset of periodic solutions [7]. Crossing H into the unstable region represents a change where the aircraft will attempt to follow a turning circle solution that is unstable (too tight) and, therefore, it loses lateral stability. The aircraft follows a periodic motion relative to the unstable turning circle solution because constant thrust is applied to the engines. Over this region in which periodic solutions exist, the velocity at which the aircraft loses lateral stability is relatively low. Crossing the curve L for small steering angles also results in a change in the type of solution that the aircraft attempts to follow. Approaching and passing the curve L from the stable region to its left, which represents large radius turning solutions, results in the aircraft attempting to follow a small radius solution instead (which is laterally unstable in this case). Similarly, crossing L from the unstable region to its right results in the aircraft starting to follow a stable large radius turn. Therefore, there is a hysteresis loop as is typical in dynamical systems with limit point bifurcations [7]. For large values of $\hat{\mu} > 40\%$ the stable region to the left of L increases and

for $\hat{\mu} > 60\%$ the dynamics become uniformly stable. This large reduction in the friction coefficient results in the aerodynamics becoming the dominant effect on the dynamics. Further details of the different types of solution and the significance of passing the different bifurcations are given in [3].

Figures 2(b) and 2(c) show two-dimensional projections of the bifurcation curves onto the $(\delta, \hat{\mu})$-plane and the $(V_x, \hat{\mu})$-plane, respectively. The $(\delta, \hat{\mu})$-plane represents the bifurcation diagram in the two parameters while the same data plotted in the $(V_x, \hat{\mu})$-plane reveals the relative positions of the bifurcation curves in terms of the forward velocity V_x. When $\hat{\mu} = 0$ the solutions are uniformly stable under variation of δ. As $\hat{\mu}$ is increased the solution branches intersect the bifurcation curves L and H. By taking parameter values that lie below these two curves the laterally unstable behaviour can be avoided. Specifically, there is a region to the left of L and H with $\delta < 3.5^\circ$ and $\hat{\mu} < 40\%$ for which no unstable behaviour can occur. Therefore, a value of $\delta = 3.5^\circ$ can provide an upper bound on the steering angle used in high velocity turns. Furthermore, the curve H can provide a guide for maintaining stable manoeuvres at higher steering angles.

4 Conclusions

Details of the equations of motion for a new mathematical model were given. A comprehensive bifurcation analysis of this model of a typical single aisle passenger aircraft was performed in terms of the steering angle and a parameter representing taxiway condition (the level of friction at the tyre-ground interface). Solution branches were computed by varying the steering angle as the continuation parameter at discrete values of the friction parameter. Loci of the bifurcations were tracked directly in the parameter plane. Overall, our results give a complete account of the possible turning dynamics of the aircraft under variation of both parameters.

The results presented here reveal how different taxiway conditions can affect the aircraft's ground dynamics. It was found that a reduction in the level of friction between the ground and the tyres can lead to the existence of a region of laterally unstable dynamics associated with a Hopf bifurcation. Limit point bifurcations were found to be associated with a hysteresis loop between high velocity large radius solutions and lower velocity laterally unstable solutions. Additionally, a steering angle of 3.5° was identified as an upper bound when making stable high-velocity turns. Furthermore, with a large reduction in the friction coefficient it was found that, counter intuitively, the region of stability for large radius turns increases.

Ongoing work focuses on the sensitivity of the results presented here to variation of additional parameters, for example, mass and thrust of the aircraft. However, there are many other parameters that are of interest, including the track-width of the main landing gears, and tyre properties. Physical phenomena associated with changes in qualitative dynamics are also the subject of ongoing studies.

Acknowledgments

This research was supported by an Engineering and Physical Sciences Research Council (EPSRC) Case Award grant in collaboration with Airbus in the UK.

5 References

[1] D.H. Klyde, T.T. Myers, R.E. Magdaleno, and J.G. Reinsberg. Identification of the dominant ground handling charactersitics of a navy jet trainer. *Journal of Guidance, Control, and Dynamics*, 25(3):546–552, May 2002.

[2] D. P. Khapane. Simulation of asymmetric landing and typical ground maneuvers for large transport aircraft. *Aerospace Science and Technology*, 7(8):611–619, December 2003.

[3] J. Rankin, E. Coetzee, B. Krauskopf, and M. Lowenberg. Nonlinear ground dynamics of aircraft: Bifurcation analysis of turning solutions. *AIAA Modeling and Simulation Technologies Conference*, AIAA-2008-6529, August 2008.

[4] E.J. Doedel, A.R. Champneys, T.F. Fairgrieve, Y.A. Kuznetsov, B. Sandstede, and X. Wang. Auto 97: Continuation software. http://indy.cs.concordia.ca/auto/, May 2001.

[5] B. Etkin. *Dynamics of Atmospheric Flight*. Wiley, 1972.

[6] M. Jeanneau. Description of aircraft ground dynamics. Garteur FM AG17 RP0412731, GARTEUR, 2004.

[7] S.H. Strogatz. *Nonlinear dynamics and chaos*. Springer, 2000.